Metallic iron nanocatalysts for the selective acetylene hydrogenation under industrial front end conditions

Journal:	*ACS Sustainable Chemistry & Engineering*
Manuscript ID	sc-2021-074558.R1
Manuscript Type:	Letter
Date Submitted by the Author:	n/a
Complete List of Authors:	Hock, Sebastian; Technische Universitat Darmstadt, Ernst-Berl-Institut, Technische Chemie II Reichel, Christina; Technische Universitat Darmstadt, Eduard-Zintl-Institut Zieschang, Anne-Marie; Technische Universitat Darmstadt, Eduard-Zintl-Institut Albert, Barbara; Technische Universitat Darmstadt, Inorganic Chemistry Rose, Marcus; Technische Universitat Darmstadt, Ernst-Berl-Institut, Technische Chemie II

Metallic iron nanocatalysts for the selective acetylene hydrogenation under industrial *front end* conditions

Sebastian Hock[1]; Christina V. Reichel[2]; Anne-Marie Zieschang[2]; Barbara Albert[2]; Marcus Rose[1,]*

AUTHOR ADDRESS

[1]Technische Universität Darmstadt, Ernst-Berl-Institut für Technische und Makromolekulare Chemie, Alarich-Weiss-Str. 8, 64287 Darmstadt, Germany

[2]Technische Universität Darmstadt, Eduard-Zintl-Institut für Anorganische Chemie und Physikalische Chemie, Alarich-Weiss-Str. 12, 64287 Darmstadt, Germany

* email address of the corresponding author: marcus.rose@tu-darmstadt.de

KEYWORDS: heterogeneous catalysis, acetylene hydrogenation, front end, iron, semi hydrogenation, iron nanoparticles

ABSTRACT: The need of nontoxic, cheap, earth-abundant catalysts, which can be sustainably produced and implemented, is essential to many processes. In this work we present unsupported iron nanoparticles as an efficient catalyst for selective acetylene hydrogenation under industrially relevant *front end* conditions. Additionally, the selectivity and the activity of this catalyst can be easily moderated by the addition of carbon monoxide. The iron nanoparticles were prepared in an environment completely free of water or air using condensed ammonia at -78 °C. State-of-the-art X-ray diffraction and scanning electron microscopy were used to determine the crystal structure, morphology and purity. The catalyst showed stable performance over several experiments and beside an agglomeration of the unsupported and unstabilized particles no changes to the catalyst were detected before and after the reactions.

INTRODUCTION

Ethylene continues to be one of the most important commodity chemicals with a global consumption of 164 million tons in 2018.[1] A key step in the primary production method via steam cracking is the removal of acetylene below 1 ppmv.[2-5] On an industrial scale, the selective hydrogenation of acetylene has been an established process for years, with two common operation methods:[2-5] *front end* and *tail end* hydrogenation, placing the

hydrogenation unit either in front of the de-methanizer or behind the de-ethanizer unit.[6-8] The main difference between these processes is that under *front end* conditions the feed contains a higher amount of hydrogen, methane and carbon monoxide rendering the reaction control more challenging.[2, 4-9] The disadvantage of the *front end* option is the lower ethylene selectivity due to the high hydrogen fraction as well as the risk of hot spot formation and hence, a more challenging process control by means of safety in order to avoid a reactor runaway by an uncontrolled temperature increase.[2, 4-9] Therefore the *tail end* process is the most commonly used and researched process.[2, 4-9] The benefit of *front end* operations are however, besides a more efficient process integration, considerably lower green oil (C_{4+} by-products) production resulting in longer catalyst cycles.[2, 4, 9]

The state-of-the-art catalysts for both process options are based on palladium nanoparticles supported on alumina pellets, which provides unrivalled catalyst activity and selectivity due to alloying with silver.[2, 5, 10] The global production of palladium is small however and the demand, especially for automotive exhaust gas catalytic converters, is high, resulting in soaring palladium prices.[11] Therefore a lot of studies have been focused on enhancing catalytic properties for palladium catalysts.[2] Effects of morphology,[12-14] support interaction,[15-18] inorganic[10, 19-21] and organic[22-24] selectivity modifiers, bi- and trimetallic palladium

catalysts[25-30] have been closely analysed and optimized. Another approach under investigation is the further optimization of more abundantly available alternatives like nickel,[31-34] copper,[7, 35-36] and gold[37-39] as catalysts for selective acetylene hydrogenation in order to compete with the palladium based ones. Over the last decades nanoparticles have been in the focus for both approaches and many studies in general.[40-41] Various results can be optimized[42-43] through nanoparticle size[44-45] morphology,[46-48] surface modifying organic ligands,[48-50] and support based interactions.[51-52] Most recent deployments on acetylene hydrogenation include Pt-Sn bimetallic nanoparticles confined in mesoporous silica walls,[53] Pd on fiberglass[54] or in microporous carbon tubes,[55] gold nanoparticles supported on Ce-Zr oxides,[38] Cu_2O nanocubes[56] and many more. The preparation of iron nanoparticles especially has led to vast improvements in activity and selectivity for many different reactions.[57-60] For the selective acetylene hydrogenation iron nanoparticles have been deployed as coating for nanocatalysts[57], embedded in metal organic frameworks[58] and in inter[59] - and bimetallic[60] nanocatalysts. In this work we show for the first time the unprecedented catalytic behaviour of unsupported ultra-pure iron nanoparticles. Under industrially relevant *front end* conditions of the gas phase selective acetylene hydrogenation the prepared nanoparticles exhibit high activity and selectivity.

RESULTS AND DISCUSSION

SYNTHESIS AND CHARACTERISATION

The Fe nanoparticles were synthesised via a method by Zieschang et al.[61] by the reduction of $FeBr_2$ with sodium in liquid ammonia. After evaporating excess of ammonia, the obtained black powder was annealed at 500 °C. The product was characterized by X-ray diffraction (XRD) measurements (**Figure 1** and **Table 1**) and confirmed crystalline Fe as product. The particle size was calculated with 86.4(9) nm using the Scherrer equation.[62]

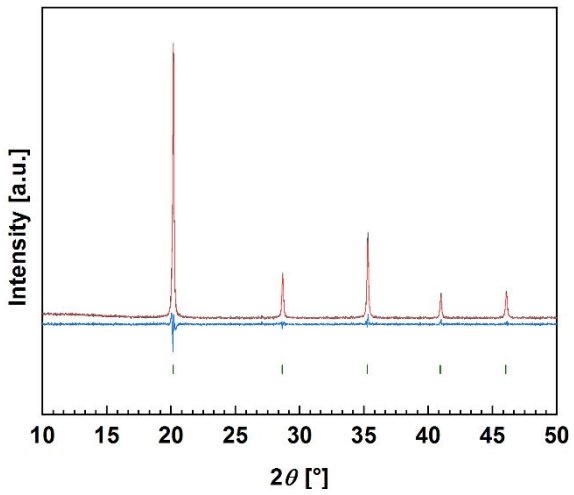

Figure 1. X-ray diffraction pattern of iron nanoparticles before catalysis after Rietveld refinement with the crystal structure of Fe *(Im-3m)*[63] (green) (black: observed, red: calculated, blue: difference curve).

Table 1. Rietveld refinement data for Fe nanoparticles before catalysis.[63]

Space group	*Im*-3*m*
Crystallite size (Lorentzian)/nm	86.4(9)
a/Å	2.8685(8)
V/Å^3	23.603(2)
R_{exp}	7.09
R_{wp}	7.73
GOF	1.09

The STEM image (**Figure 2**) shows particles with spherical dimensions and some are elongated. Few of the particles are agglomerated due to their large particle surface and magnetic behaviour. The calculated particle size according to the STEM analysis is between 80 and 100 nm. This is in good agreement with the crystallite size determined by the Scherrer equation (86.4(9) nm).

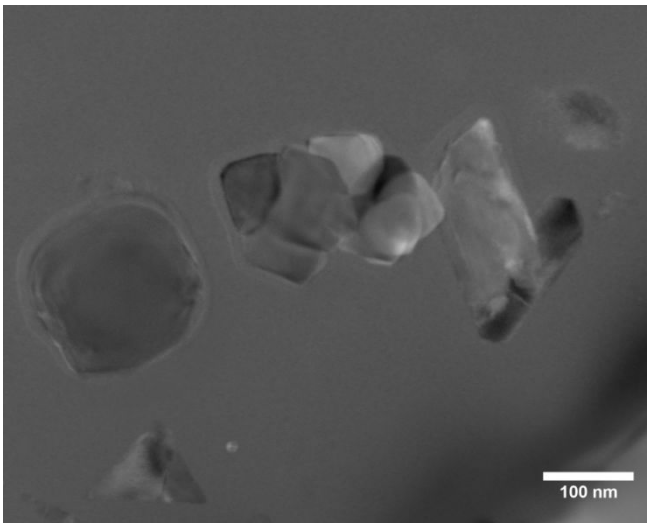

Figure 2. Oriented-dark-field STEM image of agglomerates of iron nanoparticles before catalysis.

ACETYLENE HYDROGENATION

The prepared iron nanoparticles were tested for their catalytic ability to selectively hydrogenate acetylene in a laboratory scale fixed-bed reactor setup, which was specially designed for the investigation under the industrially relevant *front end* conditions for the acetylene hydrogenation. The groundwork and general idea of the plant is based on the work of Kuhn et al.[4] and the flow sheet can be found in the supporting information **Figure S1**. For all of the experiments displayed in this work a typical feed stock of an acetylene removal unit (ARU) after Gislason et al.[64] was used (**Scheme 1**), the only simplification being that no ethane was added to the feed. Instead, the methane content was increased accordingly. Both methane

and ethane are inert in this reaction. If no ethane is added in the feed, the selectivity of the ethane formation can be more accurately determined. Additionally, a variation of the carbon monoxide content from 0 to 250 ppm was carried out to investigate if CO can also be used as a promoter of selectivity and as an inhibitor of oligomer formation for this new kind of catalyst. Propane was added to the acetylene gas cylinder as an internal standard for the GC analytics.

Scheme 1. Reaction scheme for the selective acetylene hydrogenation under front end conditions, with a typical ARU feedstock composition after Gislason et al.[64] of 25.00 mol% H_2, 0.40 mol% C_2H_2, 39.00 mol% C_2H_4, 35.25 mol% CH_4 and 0.33 mol% propane as internal standard. The CO concentration is being varied over the experiments from 0 ppm to 250 ppm.

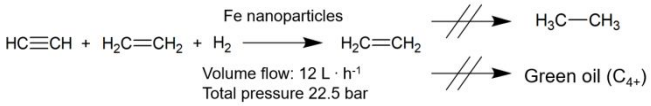

The experiments were conducted over a temperature range from 40 ˚C to 90 ˚C, which represents the industrially relevant range.[65] Starting at 40 ˚C in steps of 10 ˚C, each temperature was analysed over the course of 70 minutes reaching steady state behaviour. Then the temperature was increased by 10 ˚C at a rate of 1 ˚C · min^{-1} and the next temperature was monitored. The resulting acetylene and ethylene conversion of the experiment with 0 ppm CO

is displayed in **Figure 3** (For quicker and better comprehension of the experimental data and trends, averaged bar graph are used in this work. The original measurement data alongside the calculation of the conversion and reaction rate is shown in the **SI**). The average acetylene conversion at 40 ˚C amounted to about 3.4 % and increased to 14.3 % at 90 ˚C. The C_4 selectivity based on the acetylene conversion, fluctuated around 2 % over the howl temperature range. The ethylene conversion increased from 0.2 % at 40 ˚C to 1.1 % at 90 ˚C. Taken the 100 times higher partial pressure of ethylene in comparison to acetylene, in absolute sum more ethylene was converted than acetylene. This can be clearly observed in **Figure 4** where the reaction rate is displayed. Therefore three experiments with 50, 100 and 250 ppm CO were conducted to see if CO could be used to mediate the reaction.

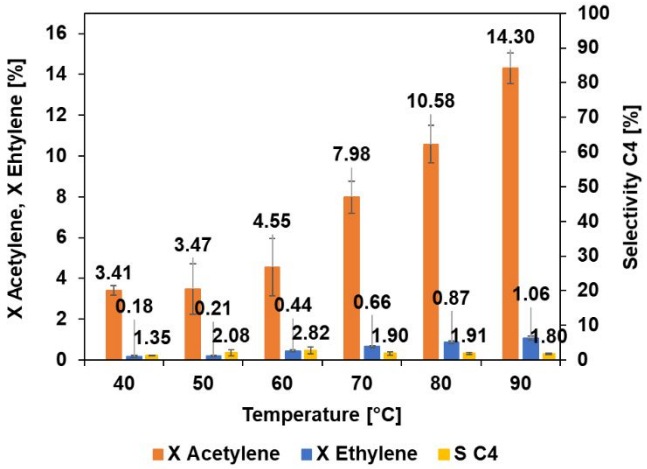

Figure 3. Temperature dependent acetylene and ethylene conversion in a temperature range from 40 ˚C to 90 ˚C using 201.9 mg of Fe nanoparticles with 0 ppm CO. The C_4 selectivity is calculated based on the acetylene conversion.

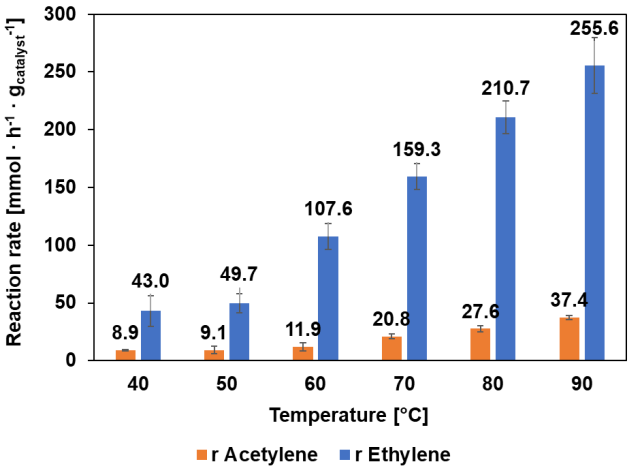

Figure 4. Acetylene and ethylene reaction rate in a temperature range from 40 ˚C to 90 ˚C using 201.9 mg of Fe nanoparticles.

The complete experimental data of the experiments with 0, 50, 100 and 250 ppm CO is given in the SI. The comparison of the conversion at a temperature of 90 ˚C is displayed in **Figure 5** the corresponding reaction rate in **Figure 6**. The results show a huge impact of the CO addition for the selectivity and activity of the catalyst. Even a relatively small amount of 50 ppm CO improves the selectivity by 90 % but also halves the acetylene conversion. At 100 ppm CO in the feed no more ethylene conversion can be observed, however the acetylene conversion is

slightly reduced as well. An increase to 250 ppm brings no benefit but lowers the acetylene conversion further. Even worse, a very small ethylene conversion is observed again at 250 ppm CO. In conclusion, the addition of carbon monoxide to the feed leads to a massive improvement in the selectivity of the Fe nanoparticles towards the acetylene conversion, but also to a decline in activity. For the investigated settings, 100 ppm CO deliver the most promising results with no observable ethane formation and still a reasonable acetylene conversion.

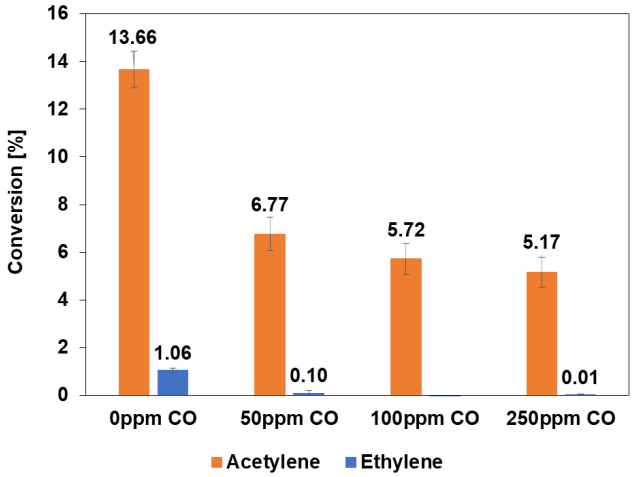

Figure 5. Comparison of the conversion of acetylene and ethylene at 90 °C reactor temperature in regard to the feed's carbon monoxide content using 201.9 mg of Fe nanoparticles.

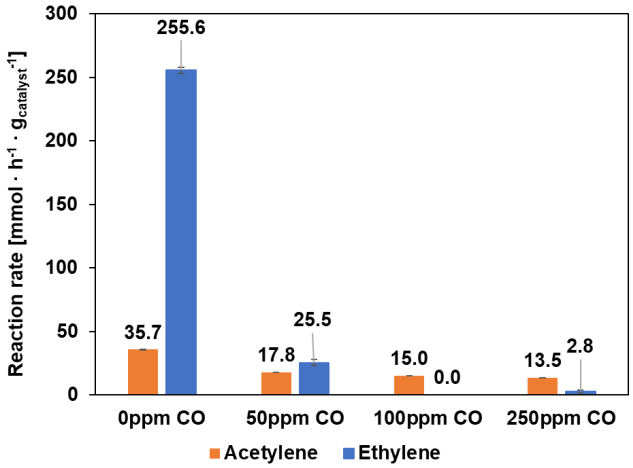

Figure 6. Comparison of the reaction rate of acetylene and ethylene at 90 ˚C reactor temperature in regard to the (feed's) carbon monoxide content using 201.9 mg of Fe nanoparticles.

A reliable comparison of the catalytic performance of the Fe nanoparticles with state-of-the-art catalysts is a challenging task, given the various amounts of possible feed compositions, reaction parameters and reporting preferences. Identical conditions could not be found in literature. However, a qualitative performance comparison proves the rather good performance of the Fe nanoparticle catalyst: One of most recent and largest comparisons by Revanchi et. al.[66] focuses on all of the possible catalyst with palladium as active metal. This represents also the current state of the art in industry, with catalyst achieving 90% and above conversion at 90˚C. The comparison of Fe nanoparticles in their current to these catalyst under similar

conditions shows room for improvement until industrial relevance is reached (**Figure 5**).[66-67] This was excpected of unsupported Fe nanoparticles in a fixed-bed reactor at 90˚C but also shows the pontential of the concept of Fe nanoparticles for the seclective acetylene hydrogenation. Further in depth research will be carried out for fitting soupports and promotors. For example compared to Ball et al.[7] SiO_2 supported AgPd and CuPd bimetallic nanoparticles, the unsuported Fe nano particles showed similar conversion as $AgPd_{0.15}/SiO_2$ and $CuPd_{0.09}/SiO_2$ at the same reaction temperature of 40˚C.[7]

CATALYST CHANGE AND STABILITY

The resulting Fe nanoparticles were characterized again after the four described experiments. After a total reaction time of 32 hours no obvious changes and differences can be seen comparing the powder diffraction patterns of the Fe nanoparticles before and after catalysis (**Figure 2** and **Figure 7**). But, the difference in the sizes of the particles with 127.7(2) nm according to the Scherrer equation after catalysis is remarkable (**Table 2**). The bigger size of the particles and crystal growth can also be seen in the STEM image (**Figure 8**). Particle growth might be caused due to thermal treatment at 90 ˚C during the catalysis and not necessarily by the reaction itself, which will be further investigated in further research.

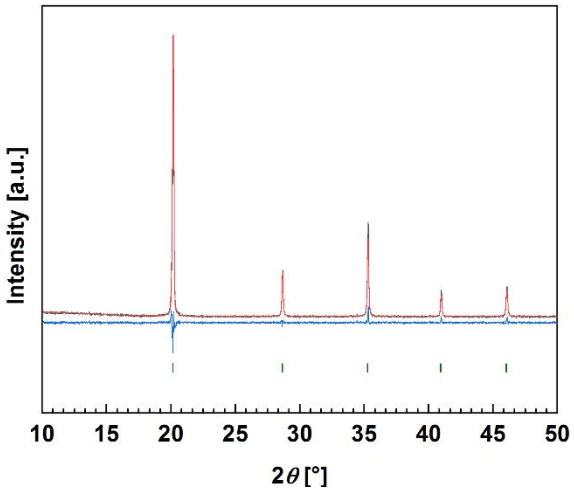

Figure 7. X-ray diffraction pattern of the iron nanoparticles after catalysis after Rietveld refinement with the structure of Fe *(Im-3m)*[63] (green) (black: observed, red: calculated, blue: difference curve).

Table 2. Rietveld refinement data for Fe nanoparticles before and after catalysis

	Pristine	**Used**
Space group	*Im-3m*	*Im-3m*
Crystallite size (Lorentzian)/nm	86.4(9)	127.7(2)
a/Å	2.8685(8)	2.8684(8)
V/Å^3	23.603(2)	23.601(2)
R_{exp}	7.09	7.25
R_{wp}	7.73	8.40

GOF	1.09	1.16

The HAADF STEM images show the Fe nanoparticles before and after catalysis experiments (**Figure 8**). An agglomeration of the Fe nanoparticles can be caused by thermal treatment or ferromagnetic behaviour. For these reasons, the determination of the particle size from the STEM images was difficult. Nevertheless, the images indicate smaller Fe nanoparticles before catalysis and bigger agglomerates afterwards. Additionally, an important information on the feasibility of the formation of Fe carbonyls can be obtained from STEM. In all experiments no quantitative Fe carbonyl formation was observed nor a catalyst mass loss. If this would have been the case then a significant surface restructuring and roughening would occur and be visible in the STEM images. Hence, at least under the applied conditions and experiment durations the catalysts seemed to be sufficiently stable. Of course, future more detailed investigations are required on the Fe carbonyl formation and loss via the gas phase in terms of stability for long periods of time-on-stream.

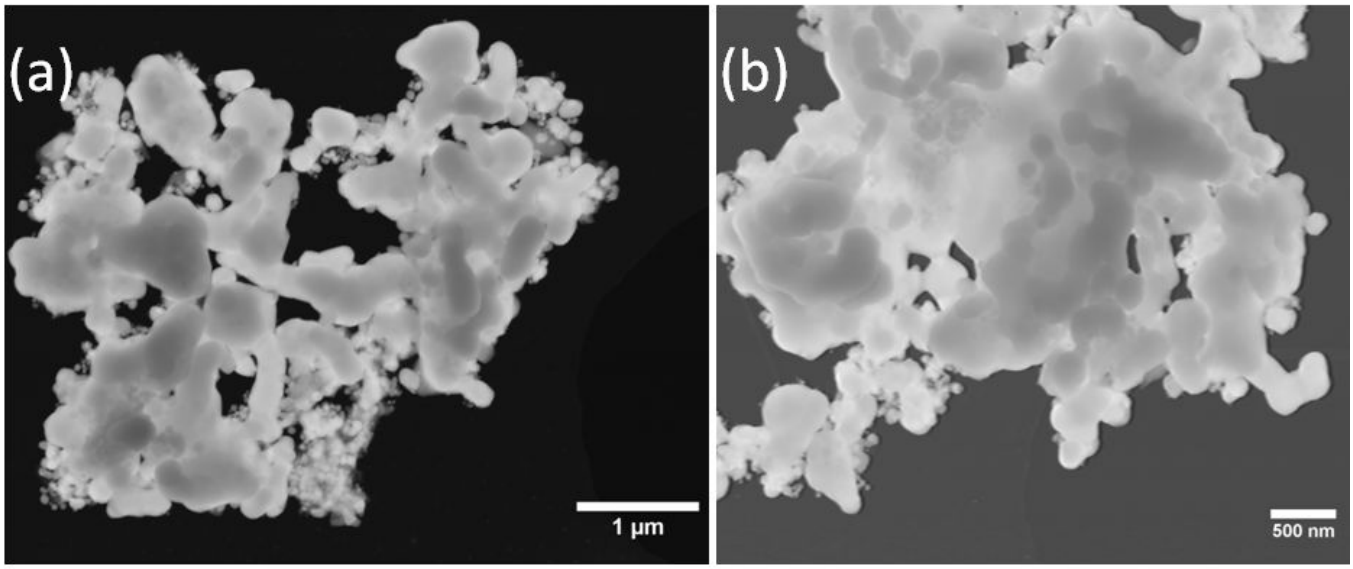

Figure 8. HAADF-STEM images of representative agglomerates of iron nanoparticles (a) before catalysis and (b) after catalysis.

CONCLUSION

In this work iron nanoparticles were prepared and used as a catalyst for the hydrogenation of acetylene under *front end* conditions. The nanoparticles were highly active and converted both acetylene and ethylene. By the addition of 100 ppm carbon monoxide the selectivity towards acetylene could be increased significantly without observable deactivation or carbonyl formation. These results indicate, that iron nanoparticles can be a suitable alternative catalyst for the selective acetylene hydrogenation even under industrially relevant reaction conditions. Overall it is proven that conventional noble metal catalysts such as in this case Pd/Ag can be

replaced by iron as an abundant, cheap and sustainable alternative. This work provides a solid foundation for further development and knowledge-based optimization of (bi-) metallic iron-based catalysts for selective gas phase hydrogenation reactions.

EXPERIMENTAL SECTION

MATERIALS

Hydrogen- (H_2, N50), hydrogen carbon monoxide mixture (0.15 mol% CO, N18; remainder H_2, N30), methane (CH_4, N25), ethylene (C_2H_4, N35), the acetylene mixture (1.2 mol% C_2H_2, N26; 1 mol% C_3H_8, N25; remainder CH_4, N25) and Argon (Ar, N50) were obtained from Air Liquid. Ammonia (NH_3, N50) was purchased from Linde, iron(II)bromide ($FeBr_2$, 98 mol%) from Sigma-Aldrich and sodium (Na, 99.5 mol%) from Riedel-De-Haën. All chemicals were used as received.

SYNTHESIS OF IRON-NANO-PARTICLES

The synthesis was carried out after Zieschang et al.[61] In order to avoid contact with oxygen or moisture during the reaction, all experiments were carried out under argon atmosphere, including the weighing of the reactants in an argon-filled glove box. Additionally, all glassware

was heated under vacuum and purged three times with argon to remove all traces of oxygen and water. The day before the reaction, ammonia (Linde; N50) was condensed into a cooling trap at -78 ˚C and dried over sodium (Riedel-De-Haën; 99.5 %) over the course of 24 hours. $FeBr_2$ (Sigma-Aldrich; 98 %) was stored in a glove box and used without further purification. $FeBr_2$ (3.86 g; 1.00 eq.) was placed in a three-necked flask and dispersed in liquid ammonia. After the addition of sodium (0.82 g; 1.9 eq.) under flowing argon, the reaction mixture immediately turned black. The suspension was kept at -78 ˚C for one hour and stirred every ten minutes. Afterwards, the reaction mixture was warmed up to room temperature to remove remaining ammonia residues. The powder was then dried in vacuo for eight hours, subsequently annealed at 500 ˚C using a defined temperature program (SI), and washed with dried methanol.[59]

SELECTIVE HYDROGENATION OF ACETYLENE

The experimental setup is displayed in the supporting information. The tubular powder reactor was fitted with a filter frit with 0.5 µm pores as support of the packed powder and an additional magnet to prevent the contamination with nanoparticles of the reactor setup. For each experiment 201.9 mg of catalyst were used and inserted under argon atmosphere. The feed specified in **Scheme 1** was realized by adding the gas mixtures listed in *MATERIALS* over the

mass flow controller network. The composition of the outlet streams was continuously measured via gas chromatography (Shimadzu GC 2010 Plus with RT-Aluminia BOND/MAPD column; 30 m; ID 0.53 mm; Film Thickness 10 µm; carrier gas Helium) every 11 minutes with a FID analyser. Before each experiment the exact feed composition was analysed over a bypass measurement for at least 60 minutes. In each experiment the temperatures 40, 50, 60, 70, 80 and 90 °C were measured for 70 minutes. In between the temperature was ramped at 1 °C · min^{-1}.

X-RAY POWDER DIFFRACTION

The X-ray powder diffraction data were obtained at room temperature by using a diffractometer with Debye-Scherrer geometry (STOE Stadi P, position-sensitive detector) with $Mo_{K\alpha 1}$ radiation (Ge(111) monochromator, λ = 0.70930 Å, glass capillary). The crystallite size was determined based on the Scherrer equation using the program TOPAS.[64]

ELECTRON MICROSCOPY

A scanning transmission electron microscope (ZEISS CrossBeam 350, EHT 30 kV) was used for characterization of the morphology of the nanoparticles. The system has STEM-in-SEM capabilities, which can give some basic bright field (BF), dark field (DF) as well some high angle annular dark field (HAADF) STEM imaging capability. The samples were prepared in a glove box and carried out on copper grids with perforated carbon films and placed on a STEM holder.

ASSOCIATED CONTENT

Supporting Information: Additional detail on the experimental plant setup and reactor, detailed experimental insights and results, temperature program used for the synthesis of Fe nanoparticles (PDF) are available in the Supporting Information.

AUTHOR INFORMATION

Corresponding Author

Marcus Rose[1,*]

*Email corresponding author: marcus.rose@tu-darmstadt.de; Tel: +4961511627290

First author (Letters from emerging scholars):

Sebastian Hock[1], PhD candidate/ doctoral student

Present Addresses

[1]Technische Universität Darmstadt, Ernst-Berl-Institut für Technische und Makromolekulare Chemie, Alarich-Weiss-Str. 8, 64287 Darmstadt, Germany

[2]Technische Universität Darmstadt, Eduard-Zintl-Institut für Anorganische Chemie und Physikalische Chemie, Alarich-Weiss-Str. 12, 64287 Darmstadt, Germany

Author Contributions

The manuscript was written through contributions of all authors. All authors have given approval to the final version of the manuscript.

Funding Sources

We gratefully acknowledge financial support by the German Research Foundation (Grant No. RO 4757/6-1).

ACKNOWLEDGMENT

The authors would like to thank Dr. Hubert Schulz (Zeiss Research Microscopy Solutions, Oberkochen) for the STEM images. M. R. and S. H. thank Martin Lucas for support with the experimental realization and adaption of the catalytic reactor for testing of the unsupported nanoparticles. The work was inspired by and carried out within the preparation of the recently granted collaborative research centre “Iron, upgraded!” (CRC 1487).

ABBREVIATIONS

ARU, Acetylene removal unit; HAADF, High-angle annular dark-field; STEM Scanning transmission electron microscope; XRD X-ray diffraction.

REFERENCES

1. Arapov, D., Optimization of SRT-VI Pyrolysis Furnaces of High-Capacity Ethylene Plant. *Theor. Found. Chem. Eng.* **2020,** *54*, 357-369. https://doi.org/10.1134/S0040579520010017

2. McCue, A. J.; Anderson, J. A., Recent advances in selective acetylene hydrogenation using palladium containing catalysts. *Front. Chem. Sci. Eng.* **2015,** *9* (2), 142-153. https://doi.org/10.1007/s11705-015-1516-4

3. Kuhn, M.; Lucas, M.; Claus, P., Long-time stability vs deactivation of pd–Ag/Al2O3 egg-shell catalysts in selective hydrogenation of acetylene. *Ind. Eng. Chem. Res.* **2015,** *54* (26), 6683-6691. https://doi.org/10.1021/acs.iecr.5b01682

4. Kuhn, M.; Lucas, M.; Claus, P., Advanced TEMKIN Reactor: Testing of industrial eggshell catalysts on the laboratory scale. *Chem. Eng. Technol.* **2015,** *38* (1), 61-67. https://doi.org/10.1002/ceat.201400616

5. Pachulski, A.; Schödel, R.; Claus, P., Kinetics and reactor modeling of a Pd-Ag/Al2O3 catalyst during selective hydrogenation of ethyne. *Appl. Catal., A* **2012,** *445*, 107-120. https://doi.org/10.1016/j.apcata.2012.08.018

6. Borodziński, A.; Bond, G. C., Selective hydrogenation of ethyne in ethene-rich streams on palladium catalysts. Part 1. Effect of changes to the catalyst during reaction. *Catal. Rev.: Sci. Eng.* **2006,** *48* (02), 91-144. https://doi.org/10.1080/01614940500364909

7. Ball, M. R.; Rivera-Dones, K. R.; Gilcher, E. B.; Ausman, S. F.; Hullfish, C. W.; Lebrón, E. A.; Dumesic, J. A., AgPd and CuPd Catalysts for Selective Hydrogenation of Acetylene. *ACS Catal.* **2020,** *10* (15), 8567-8581. https://doi.org/10.1021/acscatal.0c01536

8. Guo, Z.; Liu, Y.; Liu, Y.; Chu, W., Promising SiC support for Pd catalyst in selective hydrogenation of acetylene to ethylene. *Appl. Surf. Sci.* **2018,** *442*, 736-741. https://doi.org/10.1016/j.apsusc.2018.02.145

9. Kuhn, M.; Lucas, M.; Claus, P., Precise recognition of catalyst deactivation during acetylene hydrogenation studied with the advanced TEMKIN reactor. *Catal. Commun.* **2015,** *72*, 170-173. https://doi.org/10.1016/j.catcom.2015.10.001

10. Kim, W.-J.; Moon, S. H., Modified Pd catalysts for the selective hydrogenation of acetylene. *Catal. Today* **2012,** *185* (1), 2-16. https://doi.org/10.1016/j.cattod.2011.09.037

11. Hageluken, C., Markets for the catalyst metals platinum, palladium and rhodium. *METALL-BERLIN-* **2006,** *60* (1), 31. (no DOI available)

12. Yarulin, A.; Crespo-Quesada, R.; Egorova, E.; Kiwi-Minsker, L., Structure sensitivity of selective acetylene hydrogenation over the catalysts with shape-controlled palladium nanoparticles. *Kinet. Catal.* **2012,** *53* (2), 253-261. https://doi.org/10.1134/S0023158412020152

13. Crespo-Quesada, M.; Andanson, J.-M.; Yarulin, A.; Lim, B.; Xia, Y.; Kiwi-Minsker, L., UV–ozone cleaning of supported poly (vinylpyrrolidone)-stabilized palladium nanocubes: effect of stabilizer removal on morphology and catalytic behavior. *Langmuir* **2011,** *27* (12), 7909-7916. https://doi.org/10.1021/la201007m

14. Kim, S. K.; Kim, C.; Lee, J. H.; Kim, J.; Lee, H.; Moon, S. H., Performance of shape-controlled Pd nanoparticles in the selective hydrogenation of acetylene. *J. Catal.* **2013,** *306*, 146-154. https://doi.org/10.1016/j.jcat.2013.06.018

15. Benavidez, A. D.; Burton, P. D.; Nogales, J. L.; Jenkins, A. R.; Ivanov, S. A.; Miller, J. T.; Karim, A. M.; Datye, A. K., Improved selectivity of carbon-supported palladium catalysts for the hydrogenation of acetylene in excess ethylene. *Appl. Catal., A* **2014,** *482*, 108-115. https://doi.org/10.1016/j.apcata.2014.05.027

16. Burton, P. D.; Boyle, T. J.; Datye, A. K., Facile, surfactant-free synthesis of Pd nanoparticles for heterogeneous catalysts. *J. Catal.* **2011,** *280* (2), 145-149. https://doi.org/10.1016/j.jcat.2011.03.022

17. Riyapan, S.; Boonyongmaneerat, Y.; Mekasuwandumrong, O.; Yoshida, H.; Fujita, S.-I.; Arai, M.; Panpranot, J., Improved catalytic performance of Pd/TiO2 in the selective hydrogenation of acetylene by using H2-treated sol–gel TiO2. *J. Mol. Catal. A: Chem.* **2014,** *383*, 182-187. https://doi.org/10.1016/j.molcata.2013.12.003

18. Riyapan, S.; Boonyongmaneerat, Y.; Mekasuwandumrong, O.; Praserthdam, P.; Panpranot, J., Effect of surface Ti3+ on the sol–gel derived TiO2 in the selective acetylene hydrogenation on Pd/TiO2 catalysts. *Catal. Today* **2015,** *245*, 134-138. https://doi.org/10.1016/j.cattod.2014.07.017

19. Shin, E. W.; Kang, J. H.; Kim, W. J.; Park, J. D.; Moon, S. H., Performance of Si-modified Pd catalyst in acetylene hydrogenation: the origin of the ethylene selectivity improvement. *Appl. Catal., A* **2002,** *223* (1-2), 161-172. https://doi.org/10.1016/S0926-860X(01)00758-X

20. Shin, E. W.; Choi, C. H.; Chang, K. S.; Na, Y. H.; Moon, S. H., Properties of Si-modified Pd catalyst for selective hydrogenation of acetylene. *Catal. Today* **1998,** *44* (1-4), 137-143. https://doi.org/10.1016/S0920-5861(98)00184-9

21. Ahn, I. Y.; Kim, W. J.; Moon, S. H., Performance of La2O3-or Nb2O5-added Pd/SiO2 catalysts in acetylene hydrogenation. *Appl. Catal., A* **2006,** *308*, 75-81. https://doi.org/10.1016/j.apcata.2006.04.027

22. McKenna, F.-M.; Anderson, J. A., Selectivity enhancement in acetylene hydrogenation over diphenyl sulphide-modified Pd/TiO2 catalysts. *J. Catal.* **2011,** *281* (2), 231-240. https://doi.org/10.1016/j.jcat.2011.05.003

23. McCue, A. J.; Anderson, J. A., Sulfur as a catalyst promoter or selectivity modifier in heterogeneous catalysis. *Catal. Sci. Technol.* **2014,** *4* (2), 272-294. https://doi.org/10.1039/C3CY00754E

24. McCue, A. J.; McKenna, F.-M.; Anderson, J. A., Triphenylphosphine: a ligand for heterogeneous catalysis too? Selectivity enhancement in acetylene hydrogenation over modified Pd/TiO 2 catalyst. *Catal. Sci. Technol.* **2015,** *5* (4), 2449-2459. https://doi.org/10.1039/C5CY00065C

25. Khan, N. A.; Shaikhutdinov, S.; Freund, H.-J., Acetylene and ethylene hydrogenation on alumina supported Pd-Ag model catalysts. *Catal. Lett.* **2006,** *108* (3), 159-164. https://doi.org/10.1007/s10562-006-0041-y

26. Han, Y.; Peng, D.; Xu, Z.; Wan, H.; Zheng, S.; Zhu, D., TiO2 supported Pd@ Ag as highly selective catalysts for hydrogenation of acetylene in excess ethylene. *Chem. Commun.* **2013,** *49* (75), 8350-8352. https://doi.org/10.1039/C3CC43511C

27. Boucher, M. B.; Zugic, B.; Cladaras, G.; Kammert, J.; Marcinkowski, M. D.; Lawton, T. J.; Sykes, E. C. H.; Flytzani-Stephanopoulos, M., Single atom alloy surface analogs in Pd 0.18 Cu 15 nanoparticles for selective hydrogenation reactions. *Phys. Chem. Chem. Phys.* **2013,** *15* (29), 12187-12196. https://doi.org/10.1039/C3CP51538A

28. McCue, A. J.; Shepherd, A. M.; Anderson, J. A., Optimisation of preparation method for Pd doped Cu/Al 2 O 3 catalysts for selective acetylene hydrogenation. *Catal. Sci. Technol.* **2015,** *5* (5), 2880-2890. https://doi.org/10.1039/C5CY00253B

29. Kim, S. K.; Lee, J. H.; Ahn, I. Y.; Kim, W.-J.; Moon, S. H., Performance of Cu-promoted Pd catalysts prepared by adding Cu using a surface redox method in acetylene

hydrogenation. *Appl. Catal., A* **2011,** *401* (1-2), 12-19. https://doi.org/10.1016/j.apcata.2011.04.048

30. Osswald, J.; Kovnir, K.; Armbrüster, M.; Giedigkeit, R.; Jentoft, R. E.; Wild, U.; Grin, Y.; Schlögl, R., Palladium–gallium intermetallic compounds for the selective hydrogenation of acetylene: Part II: Surface characterization and catalytic performance. *J. Catal.* **2008,** *258* (1), 219-227. https://doi.org/10.1016/j.jcat.2008.06.014

31. Xu, Z.; Zhou, S.; Zhu, M., Ni catalyst supported on nitrogen-doped activated carbon for selective hydrogenation of acetylene with high concentration. *Catal. Commun.* **2021,** *149*, 106241. https://doi.org/10.1016/j.catcom.2020.106241

32. Zhuo, H.-Y.; Yu, X.; Yu, Q.; Xiao, H.; Zhang, X.; Li, J., Selective hydrogenation of acetylene on graphene-supported non-noble metal single-atom catalysts. *Sci. China Mater.* **2020,** *63* (9), 1741-1749. https://doi.org/10.1007/s40843-020-1426-0

33. Niu, Y.; Huang, X.; Wang, Y.; Xu, M.; Chen, J.; Xu, S.; Willinger, M.-G.; Zhang, W.; Wei, M.; Zhang, B., Manipulating interstitial carbon atoms in the nickel octahedral site for highly efficient hydrogenation of alkyne. *Nat. Commun.* **2020,** *11* (1), 1-9. https://doi.org/10.1038/s41467-020-17188-3

34. Cao, Y.; Zhang, H.; Ji, S.; Sui, Z.; Jiang, Z.; Wang, D.; Zaera, F.; Zhou, X.; Duan, X.; Li, Y., Adsorption Site Regulation to Guide Atomic Design of Ni–Ga Catalysts for Acetylene Semi-Hydrogenation. *Angew. Chem., Int. Ed.* **2020,** *132* (28), 11744-11749. https://doi.org/10.1002/anie.202004966

35. Lu, C.; Zeng, A.; Wang, Y.; Wang, A., Copper-Based Catalysts for Selective Hydrogenation of Acetylene Derived from Cu(OH)2. *ACS Omega* **2021,** *6* (4), 3363-3371. https://doi.org/10.1021/acsomega.0c05759

36. Shi, X.; Lin, Y.; Huang, L.; Sun, Z.; Yang, Y.; Zhou, X.; Vovk, E.; Liu, X.; Huang, X.; Sun, M., Copper catalysts in semihydrogenation of acetylene: from single atoms to nanoparticles. *ACS Catal.* **2020,** *10* (5), 3495-3504. https://doi.org/10.1021/acscatal.9b05321

37. Wang, J.; Xu, H.; Ao, C.; Pan, X.; Luo, X.; Wei, S.; Li, Z.; Zhang, L.; Xu, Z.-l.; Li, Y., Au@Pt Nanotubes within CoZn-Based Metal-Organic Framework for Highly Efficient Semi-hydrogenation of Acetylene. *iScience* **2020,** *23* (6), 101233. https://doi.org/10.1016/j.isci.2020.101233

38. Hua, X.; Zheng, Y.; Yang, Z.; Sun, L.; Su, H.; Murayama, T.; Qi, C., Gold Nanoparticles Supported on Ce–Zr Oxides for Selective Hydrogenation of Acetylene. *Top. Catal.* **2020**, *64* (3-4), 206-214. https://doi.org/10.1007/s11244-020-01379-9

39. Chen, H.; Li, Z.; Qin, Z.; Kim, H. J.; Abroshan, H.; Li, G., Silica-Encapsulated Gold Nanoclusters for Efficient Acetylene Hydrogenation to Ethylene. *ACS Appl. Nano Mater.* **2019**, *2* (5), 2999-3006. https://doi.org/10.1021/acsanm.9b00384

40. Witham, C. A.; Huang, W.; Tsung, C.-K.; Kuhn, J. N.; Somorjai, G. A.; Toste, F. D., Converting homogeneous to heterogeneous in electrophilic catalysis using monodisperse metal nanoparticles. *Nat. Chem.* **2010,** *2* (1), 36-41. https://doi.org/10.1038/nchem.468

41. Climent, M. J.; Corma, A.; Iborra, S., Homogeneous and heterogeneous catalysts for multicomponent reactions. *RSC Adv.* **2012,** *2* (1), 16-58. https://doi.org/10.1039/C1RA00807B

42. Tao, F. F.; Zhang, S.; Nguyen, L.; Zhang, X., Action of bimetallic nanocatalysts under reaction conditions and during catalysis: evolution of chemistry from high vacuum conditions to reaction conditions. *Chem. Soc. Rev.* **2012,** *41* (24), 7980-7993. https://doi.org/10.1039/C2CS35185D

43. Sankar, M.; Dimitratos, N.; Miedziak, P. J.; Wells, P. P.; Kiely, C. J.; Hutchings, G. J., Designing bimetallic catalysts for a green and sustainable future. *Chem. Soc. Rev.* **2012,** *41* (24), 8099-8139. https://doi.org/10.1039/C2CS35296F

44. Joo, S. H.; Park, J. Y.; Renzas, J. R.; Butcher, D. R.; Huang, W.; Somorjai, G. A., Size effect of ruthenium nanoparticles in catalytic carbon monoxide oxidation. *Nano Lett.* **2010,** *10* (7), 2709-2713. https://doi.org/10.1021/nl101700j

45. Nesselberger, M.; Ashton, S.; Meier, J. C.; Katsounaros, I.; Mayrhofer, K. J.; Arenz, M., The particle size effect on the oxygen reduction reaction activity of Pt catalysts: influence of electrolyte and relation to single crystal models. *J. Am. Chem. Soc.* **2011,** *133* (43), 17428-17433. https://doi.org/10.1021/ja207016u

46. Burda, C.; Chen, X.; Narayanan, R.; El-Sayed, M. A., Chemistry and properties of nanocrystals of different shapes. *Chem. Rev.* **2005,** *105* (4), 1025-1102. https://doi.org/10.1021/cr030063a

47. Bratlie, K. M.; Lee, H.; Komvopoulos, K.; Yang, P.; Somorjai, G. A., Platinum nanoparticle shape effects on benzene hydrogenation selectivity. *Nano Lett.* **2007,** *7*(10), 3097-3101. https://doi.org/10.1021/nl0716000

48. Wang, J.; Tan, H.; Yu, S.; Zhou, K., Morphological effects of gold clusters on the reactivity of ceria surface oxygen. *ACS Catalysis* **2015,** *5* (5), 2873-2881. https://doi.org/10.1021/cs502055r

49. Marshall, S. T.; O'Brien, M.; Oetter, B.; Corpuz, A.; Richards, R. M.; Schwartz, D. K.; Medlin, J. W., Controlled selectivity for palladium catalysts using self-assembled monolayers. *Nat. Mater.* **2010,** *9* (10), 853-858. https://doi.org/10.1038/nmat2849

50. Kwon, S. G.; Krylova, G.; Sumer, A.; Schwartz, M. M.; Bunel, E. E.; Marshall, C. L.; Chattopadhyay, S.; Lee, B.; Jellinek, J.; Shevchenko, E. V., Capping ligands as selectivity switchers in hydrogenation reactions. *Nano Lett.* **2012,** *12* (10), 5382-5388. https://doi.org/10.1021/nl3027636

51. Deng, L.; Miura, H.; Shishido, T.; Hosokawa, S.; Teramura, K.; Tanaka, T., Dehydrogenation of Propane over Silica-Supported Platinum–Tin Catalysts Prepared by Direct Reduction: Effects of Tin/Platinum Ratio and Reduction Temperature. *ChemCatChem* **2014,** *6* (9), 2680-2691. https://doi.org/10.1002/cctc.201402306

52. Singh, A. K.; Xu, Q., Synergistic catalysis over bimetallic alloy nanoparticles. *ChemCatChem* **2013,** *5* (3), 652-676. https://doi.org/10.1002/cctc.201200591

53. Maligal-Ganesh, R. V.; Pei, Y.; Xiao, C.; Chen, M.; Goh, T. W.; Sun, W.; Wu, J.; Huang, W., Sub-5 nm Intermetallic Nanoparticles Confined in Mesoporous Silica Wells for Selective Hydrogenation of Acetylene to Ethylene. *ChemCatChem* **2020,** *12* (11), 3022-3029. https://doi.org/10.1002/cctc.202000155

54. Bal'zhinimaev, B.; Paukshtis, E.; Kovalev, E., Selective Hydrogenation of Acetylene on Pd Fiberglass Catalysts. *Catal. Ind.* **2020,** *12*, 56-65. https://doi.org/10.1134/S207005042001002X

55. Guan, Q.; Zhang, J.; He, L.; Miao, R.; Shi, Y.; Ning, P., Selective Hydrogenation of Acetylene to Ethylene over the Surface of Sub-2 nm Pd Nanoparticles in Miscanthus sinensis-Derived Microporous Carbon Tubes. *ACS Sustain. Chem. Eng.* **2020,** *8* (31), 11638-11648. https://doi.org/10.1021/acssuschemeng.0c03043

56. Lu, C.; Wang, Y.; Zhang, R.; Wang, B.; Wang, A., Preparation of an Unsupported Copper-Based Catalyst for Selective Hydrogenation of Acetylene from Cu2O Nanocubes. *ACS Appl. Mater. Interfaces* **2020,** *12* (41), 46027-46036. https://doi.org/10.1021/acsami.0c12522

57. Shesterkina, A. A.; Kustov, L. M.; Strekalova, A. A.; Kazansky, V. B., Heterogeneous iron-containing nanocatalysts – promising systems for selective hydrogenation and

hydrogenolysis. *Catal. Sci. Technol.* **2020,** *10* (10), 3160-3174. https://doi.org/10.1039/D0CY00086H

58. Tejeda-Serrano, M. a.; Mon, M.; Ross, B.; Gonell, F.; Ferrando-Soria, J. s.; Corma, A.; Leyva-Pérez, A.; Armentano, D.; Pardo, E., Isolated Fe (iii)–o sites catalyze the hydrogenation of acetylene in ethylene flows under front-end industrial conditions. *J. Am. Chem. Soc.* **2018,** *140* (28), 8827-8832. https://doi.org/10.1021/jacs.8b04669

59. Armbruster, M.; Kovnir, K.; Grin, J.; Schlogl, R.; Gille, P.; Heggen, M.; Feuerbacher, M., Ordered cobalt-aluminum and iron-aluminum intermetallic compounds as hydrogenation catalysts. US8822746B2, 2014.

60. Huang, B.; Wang, T.; Yang, Z.; Qian, W.; Long, J.; Zeng, G.; Lei, C., Iron-based bimetallic nanocatalysts for highly selective hydrogenation of acetylene in N, N-dimethylformamide at room temperature. *ACS Sustain. Chem. Eng.* **2017,** *5* (2), 1668-1674. https://doi.org/10.1021/acssuschemeng.6b02413

61. Zieschang, A.-M.; Bocarsly, J. D.; Dürrschnabel, M.; Kleebe, H.-J.; Seshadri, R.; Albert, B., Low-temperature synthesis and magnetostructural transition in antiferromagnetic,

refractory nanoparticles: chromium nitride, CrN. *Chem. Mater.* **2018,** *30* (5), 1610-1616. https://doi.org/10.1021/acs.chemmater.7b04815

62. Scherrer, P., Bestimmung der Größe und der inneren Struktur von Kolloidteilchen mittels Röntgenstrahlen. *Nachrichten von der Gesellschaft der Wissenschaften zu Göttingen. Abh. Akad. Wiss. Gött., Math.-Phys. Kl.* **1918,** *2*, 98-100. http://eudml.org/doc/59018

63. Owen, E.; Yates, E., XLI. Precision measurements of crystal parameters. *London Edinburgh Philos. Mag. J. Sci.* **1933,** *15* (98), 472-488. https://doi.org/10.1080/14786443309462199

64. Gislason, J.; Xia, W.; Sellers, H., Selective hydrogenation of acetylene in an ethylene rich flow: results of kinetic simulations. *J. Phys. Chem. A* **2002,** *106* (5), 767-774. https://doi.org/10.1021/jp011238s

65. Mostoufi, N.; Ghoorchian, A.; Sotudeh-Gharebagh, R., Hydrogenation of acetylene: Kinetic studies and reactor modeling. *Int. J. Chem. React. Eng.* **2005,** *3* (1), A14. https://doi.org/10.2202/1542-6580.1215

66. Ravanchi, M. T.; Sahebdelfar, S.; Komeili, S., Acetylene selective hydrogenation: a technical review on catalytic aspects. *Rev. Chem. Eng.* **2018,** *34* (2), 215-237. https://doi.org/10.1515/revce-2016-0036

67. Dehghani, O.; Rahimpour, M. R.; Shariati, A., An experimental approach on industrial Pd-Ag supported α-Al2O3 catalyst used in acetylene hydrogenation process: Mechanism, kinetic and catalyst decay. *Processes* 2019, 7 (3), 136. https://doi.org/10.3390/pr7030136

68. *Programm TOPAS 4.2*, Bruker AXS: Karlsruhe; Germany, 2009. https://www.bruker.com/de/products-and-solutions/diffractometers-and-scattering-systems/x-ray-diffractometers/diffrac-suite-software/diffrac-topas.html (last date of access: 24.11.2021)

FOR TABLE OF CONTENTS ONLY (TOC)

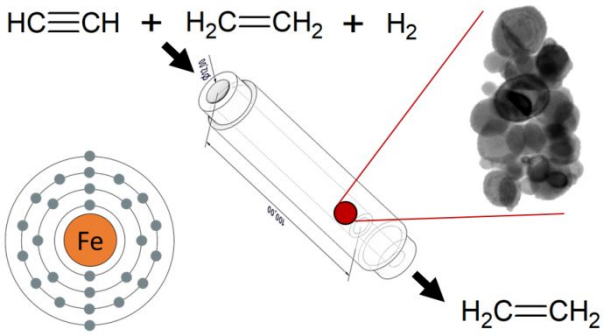

SYNOPSIS

Substituting a Pd/Ag catalyst by abundant, cheap and environmentally benign iron with a comparable catalytic performance for an industrial reaction is an essential element for sustainable chemical process development.